J|A|C|S
ARTICLES
Published on Web 12/24/2003

Effects of Spiroconjugation on the Calculated Singlet−Triplet Energy Gap in 2,2-Dialkoxycyclopentane-1,3-diyls and on the Experimental Electronic Absorption Spectra of Singlet 1,3-Diphenyl Derivatives. Assignment of the Lowest-Energy Electronic Transition of Singlet Cyclopentane-1,3-diyls

Manabu Abe,*,† Waldemar Adam,‡ Weston Thatcher Borden,*,§ Masanori Hattori,† David A. Hrovat,§ Masatomo Nojima,† Koichi Nozaki,⊥ and Jakob Wirz*,||

Contribution from the Department of Materials Chemistry and Frontier Research Center (HANDAI FRC), Graduate School of Engineering, Osaka University (HANDAI), Suita, Osaka 565-0871, Japan, Institut für Organische Chemie der Universität Würzburg, Am Hubland, D-97074 Würzburg, Germany, Department of Chemistry, Box 351700, University of Washington, Seattle, Washington 98195-1700, Department of Chemistry, Graduate School of Science, Osaka University (HANDAI), 1-16 Machikaneyama, Toyonaka, Osaka 560-0043, Japan, and Departement Chemie der Universität Basel, Klingelbergstrasse 80, CH-4056 Basel, Switzerland

Received September 3, 2003; E-mail: abe@chem.eng.osaka-u.ac.jp, borden@chem.washington.edu, j.wirz@unibas.ch

Abstract: The effect of a 2,2-ethylene-ketal functionality on the singlet−triplet energy gap (ΔE_{ST}) and on the first electronic transition in singlet cyclopentane-1,3-diyls (**1)** has been investigated. UDFT calculations predict a significant increase in the preference for a singlet ground state in the diradical with the cyclic ketal at C2 (**1g**; $\Delta E_{ST} = -6.6$ kcal/mol in C_2 symmetry and -7.6 kcal/mol in C_{2v} symmetry), compared to the 2,2-dihydroxy- and 2,2-dimethoxy-disubstituted diradicals (**1d**, $\Delta E_{ST} = -3.6$ kcal/mol in C_2 symmetry, and **1e**, $\Delta E_{ST} = -3.4$ kcal/mol in C_2 symmetry). Spiroconjugation is shown to be responsible for the larger calculated value of $|\Delta E_{ST}|$ in **1g**, relative to **1d** and **1e**. A strong correlation between the calculated values of ΔE_{ST} and the computed electronic excitation energies of the singlet diradicals is found for diradicals **1d**, **1e**, and **1g** and for 2,2-difluorocyclopentane-1,3-diyl (**1c**). A similar correlation between ΔE_{ST} and λ_{calcd} is predicted for the corresponding 1,3-diphenylcyclopentane-1,3-diyls **3**, and the predicted blue shift in the spectrum of **3g**, relative to **3e**, has been confirmed by experimental comparisons of the electronic absorption spectra of the annelated derivatives **2c**, **2e**, and **2g** in a glass at 77 K. The wavelength of the first absorption band in the singlet diradicals decreases in the order **2e** ($\lambda_{onset} = 650$ nm) > **2g** ($\lambda_{onset} = 590$ nm) > **2c** ($\lambda_{onset} = 580$ nm). The combination of these computational and experimental results provides a sound basis for reassignment of the first electronic absorption band in singlet diradicals **2c**, **2e**, and **2g** to the excitation of an electron from the HOMO to the LUMO of these 2,2-disubstituted derivatives of cyclopentane-1,3-diyl.

Introduction

Singlet diradicals are key intermediates in processes involving bond breaking and formation. In contrast to triplet diradicals such as **1a**[1] and **2b**[2], which are EPR-active and relatively long-lived, singlet diradicals are EPR-silent, and their short lifetimes make them difficult to observe and characterize.[3] Electronegative substituents (e.g., X = F or OR) make C−X bonds hyperconjugative electron acceptors, and geminal disubstitution of cyclopentane-1,3-diyls (**1**) at C2 with such substituents has been predicted to result in singlet ground states for **1c**[4] and **1d**[5]. These theoretical predictions have been confirmed experimentally by studies of the singlet diradicals **2c**, **2e**, and **2f**,[6] which were found

† Graduate School of Engineering, Osaka University.
‡ Universität Würzburg.
§ University of Washington.
⊥ Graduate School of Science, Osaka University.
|| Universität Basel.

(1) (a) Buchwalter, S. L.; Closs, G. L. *J. Am. Chem. Soc.* **1975**, *97*, 3857−3858. (b) Buchwalter, S. L.; Closs, G. L. *J. Am. Chem. Soc.* **1979**, *101*, 4688−4694.
(2) (a) Adam, W.; Harrer, H. M.; Kita, F.; Nau, W. M. *Adv. Photochem.* **1998**, *24*, 205−254. (b) Kita, F.; Adam. W.; Jordan, P.; Nau, W. M.; Wirz, J. *J. Am. Chem. Soc.* **1999**, *121*, 9265−9275.
(3) (a) Pederson, S.; Herek, J. L.; Zewail, A. H. *Science* **1994**, *266*, 294−309. (b) De Feyter, S.; Diau, E. W.-G.; Zewail, A. H. *Angew. Chem., Int. Ed.* **2000**, *39*, 260−263.
(4) (a) Xu, J. D.; Hrovat, D. A.; Borden, W. T. *J. Am. Chem. Soc.* **1994**, *116*, 5425−5427. (b) Getty, S. J.; Hrovat, D. A.; Borden, W. T. *J. Am. Chem. Soc.* **1994**, *116*, 1521−1527. (c) Borden, W. T. *Chem. Commun.* **1998**, 1919−1925
(5) Abe, M.; Adam, W.; Nau, W. M. *J. Am. Chem. Soc.* **1998**, *120*, 11304−11310.
(6) (a) Adam, W.; Borden, W. T.; Burda, C.; Foster, H.; Heidenfelder, T.; Jeubes, M.; Hrovat, D. A.; Kita, F.; Lewis, S. B.; Scheutzow, D.; Wirz, J. *J. Am. Chem. Soc.* **1998**, *120*, 593−594. (b) Abe, M.; Adam, W.; Heidenfelder, T.; Nau, W. M.; Zhang, X. *J. Am. Chem. Soc.* **2000**, *122*, 2019−2026. (c) Abe, M.; Adam, W.; Hara, M.; Hattori, M.; Majima, T. Nojima, M.; Tachibana, K.; Tojo, S. *J. Am. Chem. Soc.* **2002**, *124*, 6540−6541.

10.1021/ja038305b CCC: $27.50

Table 1. Calculated Singlet−Triplet Energy Gaps ($\Delta E_{ST} = E_S - E_T$) and Excitation Wavelengths and Energies of Cyclopentane-1,3-diyls **1**

		ΔE_{ST} (kcal/mol)[a] ($\langle S^2_S\rangle$, ΔE_{ST}^{corr})			λ_{calcd} (nm)[b]		excitation energies (kcal/mol)[b]	
1	X	C_2	C_{2v}	lit.	C_2 (f)[c]	C_{2v} (f)[c]	C_2	C_{2v}
1a	H		+0.64 (1.01, +1.3)	+1.2[d]		1148 (0.14)		24.9
1c	F		−7.1 (0.77, −11.4)	−9.8[e]		368.4 (0.39)		77.6
1d	OH	−3.6[f] (0.87, −6.4)						
1e	OMe	−3.4[f] (0.88, −6.1)			424.1 (0.32)		68.8	
1g	−O(CH$_2$)$_2$O−	−6.6 (0.77, −10.7)	−7.6 (0.75, −12.2)		397.6 (0.33)	390.7 (0.34)	71.9	73.2

[a] Calculations were performed at the UB3LYP/6-31G* level of theory. The values in parentheses indicate the $\langle S^2_S\rangle$ values for the singlet state and the energy gaps computed after correction for spin contamination in the singlet (ΔE_{ST}^{corr}), by using Yamaguchi's formula (ref 19); $\Delta E_{ST}^{corr} = \langle S^2_T\rangle/(\langle S^2_T\rangle - \langle S^2_S\rangle) \times \Delta E_{ST}$. The $\langle S^2_T\rangle$ values for the triplet state were calculated to be ca. 2.0; see Supporting Information. [b] Absorption wavelengths and excitation energies were calculated at the RCIS/6-31+G*//UB3LYP/6-31G* level of theory. [c] Calculated oscillator strengths. [d] In C_2 symmetry at the CISD level of theory; ref 20. [e] In C_{2v} symmetry at the CASPT2N level of theory; ref 4a. [f] Substituents (H or Me) on both oxygen atoms are exo to the cyclopentane ring.

to be relatively long-lived, with lifetimes of up to 1 μs at room temperature. Each of these three singlet diradicals was also discovered to exhibit an intense absorption band in the visible region.

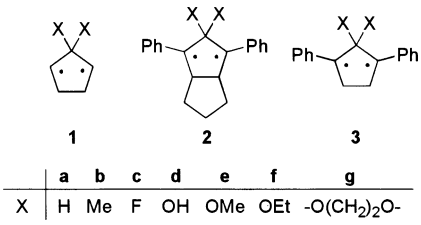

The kinetic stability of **2c**, **2e**, and **2f** has provided opportunities to investigate the chemical behavior and electronic character of these localized singlet 1,3-diradicals.[7−9] The possibility of performing experiments on **2c**, **2e**, and **2f** has, in turn, motivated additional calculations.[10,11] In the context of these ongoing experimental and computational studies, we have investigated the effects of different C2[6a,b] and *p*-phenyl[6c] substituents on the chemistry and spectroscopy of the singlet diradicals **1** and **2**.

For the seemingly inconsequential replacement of either the hydroxy substituents in **1d** or the methoxy substituents in **1e** with ethylene-ketal in **1g**, our calculations have predicted unexpectedly large effects on both the singlet−triplet energy gap ($\Delta E_{ST} = E_S - E_T$) and on the wavelength (λ) of the first electronic absorption band of the singlet diradicals. The surprising substituent effect, calculated for **1g**, prompted us to generate the diradical **2g** to test these predictions.

Here we report the results of this combined theoretical and experimental study. Our calculations and experiments not only reveal a new type of substituent effect on both ΔE_{ST} and λ in singlet 2,2-disubstituted cyclopentane-1,3-diyls, but also provide a definitive assignment of the lowest-energy electronic transition in the singlet diradicals **2c** and **2e**−**g**. These findings have led us to correct our earlier tentative assignment of the long-wavelength absorption band of **2c**, from being due to a parity-forbidden absorption of its benzyl chromophores[6a] to being caused by the excitation of an electron from the HOMO to the LUMO of this singlet 2,2-difluorocyclopentane-1,3-diyl derivative.

Computational Methodology

Geometry optimizations and calculations of the energy gap (ΔE_{ST}) were performed with the 6-31G* basis set,[12] using Becke's hybrid, three-parameter functional[13] and the nonlocal correlation functional of Lee, Yang, and Parr (B3LYP).[14] Excitation energies were computed by RCIS[15] or time-dependent density functional theory (TD-RB3LYP)[16] with either the 6-31G*[12] or the 6-31+G*[17] basis set. All of the calculations were carried out with the Gaussian 98 suite of programs.[18] Optimized geometries and energies for all the molecules discussed in this paper are available as Supporting Information.

Results and Discussion

Calculated Effect on ΔE_{ST} of the Ethylene Ketal Functionality at C2 in 1g. The singlet−triplet energy gaps (ΔE_{ST}) of cyclopentane-1,3-diyls **1c**−**g** were calculated at the UB3LYP/6-31G* level of theory (Table 1). UB3LYP calculations generally give values of ΔE_{ST} that are too small in magnitude when they are compared to the values obtained from high-level ab initio calculations. For example, the UB3LYP/6-31G* calculations on **1c** give a value of $\Delta E_{ST} = -7.1$ kcal/mol, which is 2.7 kcal/mol smaller in magnitude than that obtained by CASPT2/6-31G* calculations.[4a]

The tendency for UB3LYP calculations to underestimate the magnitudes of ΔE_{ST} values is due to the fact that unrestricted "singlet" wave functions are actually mixtures of the wave functions for pure singlet and triplet states. For example, the

(7) For studies of boron-centered singlet cyclobutane-1,3-diyls, see: (a) Scheschkewitz, D.; Amii, H.; Gornitzka, H.; Schoeller, W. W.; Bourissou, D.; Bertrand, G. *Science* **2002**, *295*, 1880−1881. (b) Wentrup, C. *Science* **2002**, *295*, 1846−1847.
(8) For studies of singlet 1,3-diphosphacyclobutane-2,4-diyls, see: (a) Grutzmacher, H.; Breher, F. *Angew. Chem., Int. Ed.* **2002**, *41*, 4006−4011. (b) Schoeller, W. W.; Begemann, C.; Niecke, E.; Gudat, D. *J. Phys. Chem. A* **2001**, *105*, 10731−10738. (c) Niecke, E.; Fuchs, A.; Baumeister, F.; Martin Nieger, Schoeller, W. W. *Angew. Chem., Int. Ed. Engl.* **1995**, *34*, 555−557.
(9) For reviews of non-Kekulé diradicals with singlet ground states, see: (a) Borden, W. T.; Iwamura, H.; Berson, J. A. *Acc. Chem. Res.* **1994**, *27*, 109−116. (b) Berson, J. A. *Acc. Chem. Res.* **1997**, *30*, 238−244.
(10) Abe, M.; Ishihara, C.; Nojima, M. *J. Org. Chem.* **2003**, *68*, 1618−1621.
(11) Zhang, D. Y.; Hrovat, D. A.; Abe, M.; Borden, W. T. *J. Am. Chem. Soc.* **2003**, *125*, 12823−12828.
(12) Hariharan, P. C.; Pople, J. A. *Theor. Chim. Acta* **1973**, *28*, 213−222.
(13) Becke, A. D. *J. Chem. Phys.* **1993**, *98*, 5648−5652.
(14) Lee, C.; Yang, W.; Parr, R. G. *Phys. Rev. B* **1988**, *37*, 785−789.
(15) Foresman, J. B.; Head-Gordon, M.; Pople, J. A.; Frisch, M. J. *J. Phys. Chem.* **1992**, *96*, 135−149.
(16) (a) Stratmann, R. E.; Scuseria, G. E.; Frisch, M. J. *J. Chem. Phys.* **1998**, *109*, 8218−8224. (b) Casida, M. E.; Jamorksi, C.; Casida, K. C.; Salahub, D. R. *J Chem. Phys.* **1998**, *108*, 4439−4449.
(17) Frisch, M. J.; Pople, J. A.; Binkley, J. S. *J. Chem. Phys.* **1984**, *80*, 3265−3269.
(18) Frisch, M. J.; Trucks, G. W.; Schlegel, H. B.; Scuseria, G. E.; Robb, M. A.; Cheeseman, J. R.; Zakrzewski, V. G.; Montgomery, J. A., Jr.; Stratmann, R. E.; Burant, J. C.; Dapprich, S.; Millam, J. M.; Daniels, A. D.; Kudin, K. N.; Strain, M. C.; Farkas, O.; Tomasi, J.; Barone, V.; Cossi, M.; Cammi, R.; Mennucci, B.; Pomelli, C.; Adamo, C.; Clifford, S.; Ochterski, J.; Petersson, G. A.; Ayala, P. Y.; Cui, Q.; Morokuma, K.; Malick, D. K.; Rabuck, A. D.; Raghavachari, K.; Foresman, J. B.; Cioslowski, J.; Ortiz, J. V.; Stefanov, B. B.; Liu, G.; Liashenko, A.; Piskorz, P.; Komaromi, I.; Gomperts, R.; Martin, R. L.; Fox, D. J.; Keith, T.; Al-Laham, M. A.; Peng, C. Y.; Nanayakkara, A.; Gonzalez, C.; Challacombe, M.; Gill, P. M. W.; Johnson, B. G.; Chen, W.; Wong, M. W.; Andres, J. L.; Head-Gordon, M.; Replogle, E. S.; Pople, J. A. *Gaussian 98*, revision A 11.3; Gaussian, Inc.: Pittsburgh, PA, 1998.

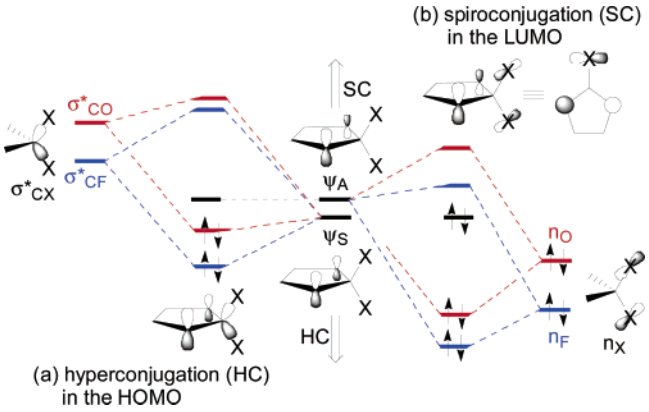

Figure 1. Orbital interaction diagram for a cyclopentane-1,3-diyl, disubstituted at C2 with X = F or X = OR, showing (a) hyperconjugation (HC) of the symmetric combination of the 2p-π AOs at C1 and C3 (ψ_S) with the pseudo π combination of the antibonding C−X σ^* orbitals at C2. (b) Spiroconjugation (SC) of the pseudo-π combination of 2p nonbonding AOs on X (n_X) with the antisymmetric combination of 2p-π AOs at C1 and C3 (ψ_A). The greater electronegativity of fluorine relative to oxygen should make HC more important for X = F than for X = OR in determining the energy of the HOMO. However, at a C_{2v} geometry, where n_O is properly aligned for maximal interaction with ψ_A, the greater electronegativity of fluorine relative to oxygen should make SC more important for X = OR than for X = F in determining the energy of the LUMO.

value of $S^2_S = 0.77$ for the UB3LYP "singlet" wave function for **1c** is intermediate between the values of $S^2_S = 0.00$ for a pure singlet and $S^2_T = 2.00$ for a pure triplet.

Houk and Yamaguchi have proposed a simple formula to correct values of ΔE_{ST}, obtained using unrestricted wave functions, for the effects of spin contamination.[19] As shown in Table 1, the corrected UB3LYP value of $\Delta E_{ST} = -11.4$ kcal/mol for **1c** is 1.6 kcal/mol larger in magnitude than the CASPT2 value but closer to it than is the uncorrected UB3LYP value of $\Delta E_{ST} = -7.1$ kcal/mol. The same type of bracketing of the CASPT2 value of ΔE_{ST} has also been found in the results of UB3LYP and CASPT2 calculations on the 1,3-diphenyl derivative of **1c**.[11]

Since the results in Table 1 show the same trends whether the corrected or uncorrected UB3LYP values of ΔE_{ST} are used, for simplicity, the following discussion is based on the uncorrected values. No matter which set of values is employed, $|\Delta E_{ST}$ **(1c)**$| \gg |\Delta E_{ST}$ **(1d)**$| \sim |\Delta E_{ST}$ **(1e)**$|$, and $|\Delta E_{ST}$ **(1c)**$|$ is midway between the C_2 and C_{2v} values of $|\Delta E_{ST}$ **(1g)**$|$. Since a pair of oxygen substituents is attached to C2 in **1d**, **1e**, and **1g**, the finding that $|\Delta E_{ST}$ **(1g)**$| \gg |\Delta E_{ST}$ **(1d)**$|$ and $|\Delta E_{ST}$ **(1e)**$|$ is quite surprising.

The singlet ground states that have been predicted and found for 2,2-difluoro- and 2,2-dialkoxycyclopentane-1,3-diyls **1** and **2**[4−6,10,11] have been attributed to hyperconjugation (HC), involving the C−X bonds of the electronegative substituents at C2. The symmetric combination of the 2p-π AOs at C1 and C3 (ψ_S) can donate electron density into the pseudo π combination of the low-lying antibonding C2-X σ^* orbitals. As shown schematically in Figure 1a, this interaction stabilizes ψ_S relative to the antisymmetric combination of the 2p-π AOs at C1 and C3 (ψ_A), because ψ_A has the wrong symmetry for interaction with either the σ or σ^* orbitals of the C−X bonds at C2. The stronger the HC between ψ_S and the antibonding C2-X σ^* orbitals, the greater the stabilization of ψ_S relative to ψ_A and, hence, of the singlet relative to the triplet.

As depicted graphically in Figure 1, the greater electronegativity of fluorine, compared to oxygen, results in σ_{C-F}^* orbitals being lower in energy than σ_{C-O}^* orbitals. The lower the energy of the σ_{C-X}^* pseudo π orbitals, the stronger their HC with ψ_S and the greater the stabilization of the singlet relative to the triplet. Thus, the larger calculated magnitude of $|\Delta E_{ST}|$ in **1c** (X = F) than that in **1d** (X = OH) or **1e** (X = OMe) is easily understood. However, the unexpected finding, that the ethylene-ketal functionality (X,X = $-O(CH_2)_2O-$) at C2 in **1g** stabilizes the singlet state relative to the triplet, as much or more than the pair of fluorine atoms in **1c**, indicates that, in addition to HC, another factor plays a role in determining ΔE_{ST}. As shown in Figure 1 and as discussed below, we propose that this additional factor is spiroconjugation (SC)[21] of the pseudo-π combination of 2p nonbonding AOs on the oxygen atoms (n_O) with the antisymmetric combination of 2p-π AOs at C1 and C3 (ψ_A). SC stabilizes the lone pair of electrons n_O but destabilizes ψ_A. Consequently, like HC, SC increases the energy difference between ψ_S and ψ_A and, thus, increases the magnitude of ΔE_{ST}.

Since SC in **1g** involves the 2p nonbonding AOs on oxygen, SC should be sensitive to the spatial orientation of these AOs. SC of n_O with ψ_A should be strongest at a geometry where the nodal planes of these two orbitals are coincident. The expected conformational dependence of SC would explain why ΔE_{ST} is larger at an idealized C_{2v} geometry of **1g** than at the C_2 equilibrium geometries of the singlet and triplet states and why ΔE_{ST} is larger in **1g** than in **1d** and **1e**. Diol **1d** and dimethyl ketal **1e** both lack the ethano bridge that is present in the ethylene ketal **1g**. Without this constraint, the n_O orbitals at the equilibrium geometries of **1d** and **1e** are less well aligned than the n_O orbital in **1g** for SC with ψ_A (vide infra).

To confirm the dependence of ΔE_{ST} on the conformations about the C2−O bonds in **1d**, **1e**, and **1g**, the effect of synchronous changes in both O−C2−O−H dihedral angles (θ) on ΔE_{ST} was calculated for diradical **1d** (X = OH). The geometry optimizations at $\theta = 0$ and 180° were performed in C_{2v} symmetry. For the other C2−O conformations, C_2 symmetry was maintained in the optimizations. A plot of ΔE_{ST} versus θ in **1d** is given in Figure 2a.

As shown in Figure 2a, ΔE_{ST} is calculated to depend strongly on the dihedral angle θ. The orientation of the 2p AOs on the oxygen atoms (n_O) affects ΔE_{ST} in the manner expected on the basis of SC. The most negative values of ΔE_{ST} occur at dihedral angles of $\theta = 0$ and 180°, where the spiroconjugative interaction between n_O and ψ_A is the strongest. The size of $|\Delta E_{ST}|$ is smallest at a dihedral angle of $\theta = 90°$, where n_O lies in the nodal plane of ψ_A, so that the spiroconjugative interaction between them vanishes. The degree to which n_O mixes with ψ_A is apparent from the plots in Figure 3 of the lowest unfilled (LU)MO in **1d** at these three dihedral angles.

The same type of dependence of ΔE_{ST} on the O−C2−O−CH_3 dihedral angle was also calculated for **1e** (X = OCH_3). The uncorrected singlet−triplet energy gaps were found to be $\Delta E_{ST} = -7.2$ kcal/mol at $\theta = 0°$, $\Delta E_{ST} = -3.4$ kcal/mol at $\theta = 90°$, and $\Delta E_{ST} = -5.1$ kcal/mol at $\theta = 180°$.

(19) (a) Yamaguchi, K.; Jensen, F.; Dorigo, A.; Houk, K. N. *Chem. Phys. Lett.* **1988**, *149*, 537. (b) Soda, T.; Kitagawa, Y.; Onishi, H.; Takano, Y.; Shigeta, Y.; Nagao, H.; Yoshioka, Y.; Yamaguchi, K. *Chem. Phys. Lett.* **2000**, *319*, 223−230.
(20) Sherrill, C. D.; Seidl, E. T.; Schaefer, H. F., III. *J. Phys. Chem.* **1992**, *96*, 3712−3716.
(21) Simmons, H. E.; Fukunaga, T. *J. Am. Chem. Soc.* **1967**, *89*, 5208−5215.

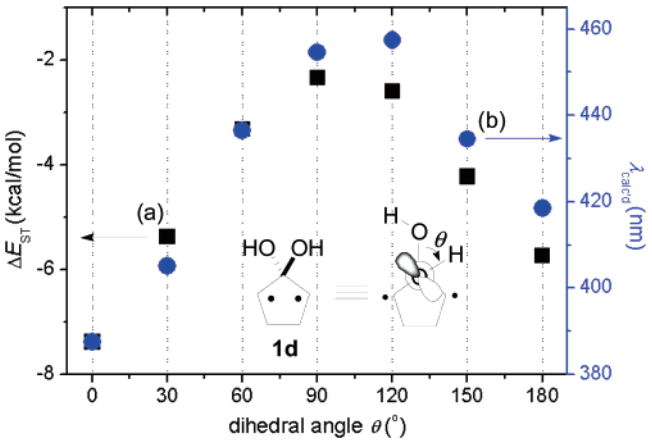

Figure 2. Effect of synchronous changes in both O−C2−O−H dihedral angles (θ) in 2,2-dihydroxycyclopentane-1,3-diyl (**1d**) on (a) the calculated singlet−triplet energy gap (ΔE_{ST}) (■) and (b) the calculated absorption wavelength (λ_{calcd}) (blue ●).

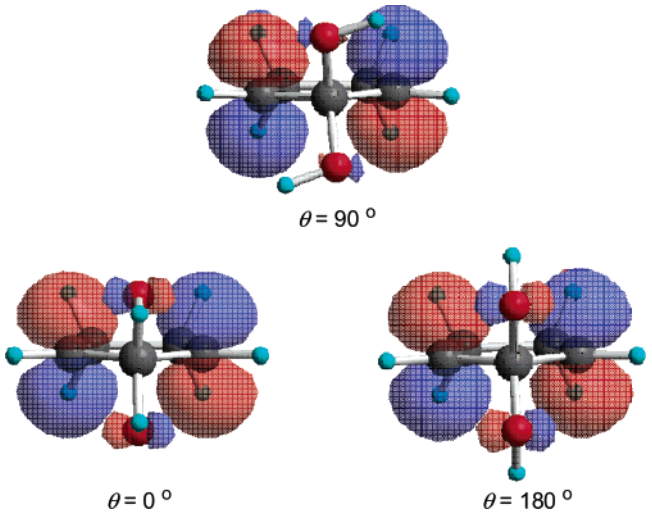

Figure 3. Boundary-surface plots of the LUMO of **1d** (RB3LYP/6-31G*//UB3LYP/6-31G*) at $\theta = 0$, 90, and 180°. The plots show that n_O mixes with ψ_A at $\theta = 0°$ and 180° but not at 90°. The small contribution of oxygen to the LUMO at $\theta = 90°$ comes largely from the lone pairs on oxygen that occupy hybrid AOs, rather than the pure 2p AOs that comprise n_O.

The uncorrected values of ΔE_{ST} in **1d**, plotted as a function of the O−C2−O−H dihedral angles (θ) in Figure 2a, mirror the uncorrected values of ΔE_{ST} in Table 1 at the optimized geometries of the singlet ground states[22] of **1d** ($\theta = 51.2°$), **1e** ($\theta = 61.8°$), **1g** ($\theta = 12.0°$), and **1g** when this diradical is constrained to have C_{2v} symmetry ($\theta = 0.0°$). This correspondence shows that the differences between the values of ΔE_{ST} for **1d**, **1e**, and **1g** in Table 1 are largely due to the different values of θ at the equilibrium geometry of each of these oxygen-substituted singlet diradicals. The O−C2−O−H dihedral angles control the degree of SC between n_O and ψ_A, and the mixing between these two orbitals modulates the energy of the LUMO, which, in turn, affects the size of ΔE_{ST}.

Since the fluorine atoms in **1c** also have a lone pair of electrons in an orbital (n_F) that can mix with ψ_A, SC, as well as HC, presumably plays a role in determining the size of ΔE_{ST} in **1c**. As shown schematically in Figure 1, the greater electronegativity of fluorine, compared to oxygen, presumably makes the effect of HC on lowering the energy of the HOMO larger for X = F than for X = OR. However, at a C_{2v} geometry, where n_O is aligned for maximal interaction with ψ_A, the greater electronegativity of fluorine relative to oxygen should make the effect of SC on raising the energy of the LUMO more important for X = OR than for X = F.

Table 1 shows that, when the geometry of **1g** is constrained to have C_{2v} symmetry, the calculated value of $|\Delta E_{ST}|$ is larger than that computed for **1c**. Therefore, it appears that the larger effect of oxygen on SC in the LUMO dominates the larger effect of fluorine on HC in the HOMO, when the n_O orbital is properly oriented for maximal interaction with ψ_A.

It should be noted that only at $\theta = 0$ and 180° is n_O orthogonal to ψ_S. At $\theta = 90°$, where n_O is orthogonal to ψ_A, n_O is best oriented to mix with and destabilize ψ_S. Therefore, the O−C2−O−R dihedral angles in **1d**, **1e**, and **1g** affect $|\Delta E_{ST}|$ by modulating the energy of not only the LUMO but also of the HOMO. To assess quantitatively the dihedral angle dependence of the HOMO and LUMO energies in **1d**, the energies of these Kohn−Sham orbitals were calculated at different values of θ for the singlet state at the RB3LYP/6-31G*//UB3LYP/6-31G* level of theory. The results of these calculations are displayed in Figure 4.[23]

As shown in Figure 4a, the LUMO energy of **1d** depends strongly on the angle θ. The maximum energy is calculated to occur at an angle of 0° ($\Delta E^{LUMO} \equiv 0$ kcal/mol); but, surprisingly, the energy minimum for the LUMO is found not at $\theta = 90°$ but at a dihedral angle of $\theta = 120°$ ($\Delta E^{LUMO} = -12.0$ kcal/mol). The LUMO energy is rather insensitive to θ for $\theta > 90°$, where the protons of both hydroxy groups are endo to the cyclopentane ring, but the energy of the LUMO increases sharply with decreasing values of θ for $\theta < 90°$.

The asymmetry about $\theta = 90°$ of the plot of ΔE^{LUMO} versus θ in Figure 4a indicates that ψ_A is stabilized when the protons of both hydroxy groups are endo to the cyclopentane ring. This suggests the existence of an electrostatic interaction between the electrons in the 2p-π AOs on C1 and C3 and the protons of the hydroxy groups in the endo conformers ($\theta > 90°$). Such an interaction may be the reason why the LUMO energy shows a minimum at 120°. At this angle, each proton is close to one of the 2p-π AOs. Without this type of interaction, ΔE^{LUMO} should be the same at $\theta = 120°$ as at $\theta = 60°$, rather than being 4.6 kcal/mol lower at $\theta = 120°$.

As expected, the variation of the HOMO energy of **1d** with the dihedral angle θ (Figure 4b) is opposite to the LUMO (Figure 4a). In going from $\theta = 0°$ to $\theta = 90°$, the HOMO energy increases by 4.3 kcal/mol. As already noted, at $\theta = 90°$, n_O is optimally oriented to interact with ψ_S via SC, and this mixing destabilizes the HOMO of **1d**. The interaction between n_O and ψ_S at $\theta = 90°$ is illustrated schematically in Figure 5a, and a boundary surface plot of the HOMO at $\theta = 90°$ is shown in Figure 5b.

From $\theta = 90°$, the HOMO energy of **1d** decreases by 8.4 kcal/mol to a minimum at $\theta = 180°$ ($\Delta E^{HOMO} = -4.1$ kcal/mol). The asymmetry about $\theta = 90°$ in the plot of the HOMO

(22) At the optimized geometries of the triplet states, the dihedral angles θ were calculated to be $\theta = 58.2°$ (**1d**), 63.2° (**1e**), and 12.7° (**1g**). The smaller dihedral angle at the optimized geometry of each singlet state is consistent with SC stabilization of the singlet.

(23) A similar dihedral angle dependence of the energies of the two singly occupied orbitals was found in UB3LYP/6-31G* calculations on the triplet state of **1d**. Since the energies plotted in Figure 4 are those of Kohn−Sham orbitals, the changes in the energies of these orbitals are only qualitatively related to the change in ΔE_{ST} that are plotted in Figure 2.

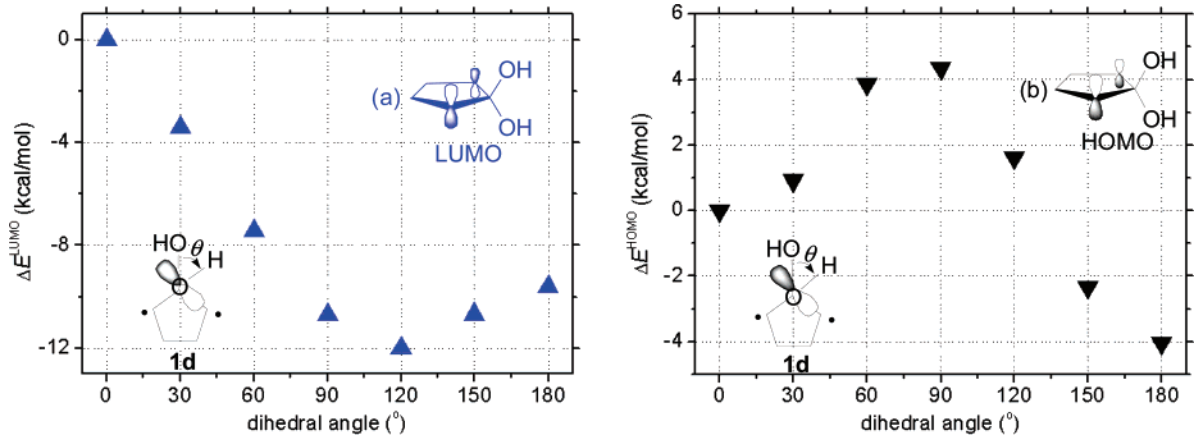

Figure 4. Effect of synchronous changes in both O−C2−O−H dihedral angles (θ) on the energies (a) of the LUMO (blue ▲) and (b) of the HOMO (▼) in **1d**. The energy scales in the two plots differ, because the change in ΔE^{LUMO} is 50% larger than that in ΔE^{HOMO}.

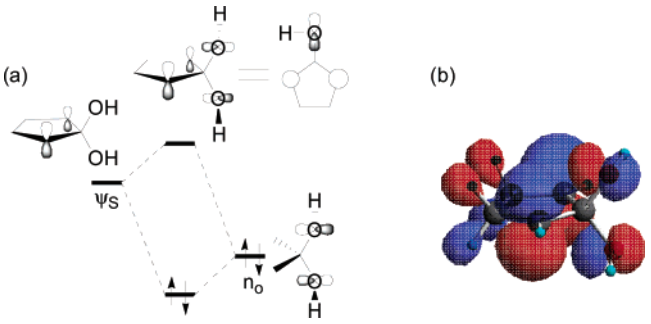

Figure 5. (a) Spiroconjugation (SC) between n_O and ψ_S at $\theta = 90°$ and (b) a boundary-surface plot of the HOMO at this dihedral angle, showing the effect of the mixing between n_O and ψ_S by spiroconjugation.

energy versus the O−C2−O−H dihedral angle suggests that an electrostatic interaction between the electrons in the carbon 2p-π AOs and the protons of the endo hydroxy groups tends to stabilize not only the LUMO but also the HOMO of **1d**.

The dihedral-angle (θ) dependence of the spiroconjugation (SC) effect on the HOMO and LUMO energies of the exo,exo conformers of **1d** ($0° < \theta < 90°$) (Figure 4) accounts qualitatively for the increase of 3.0 kcal/mol in the uncorrected magnitudes of ΔE_{ST} (Table 1) on replacing the dimethyl ketal in **1e** ($\theta = 61.8°$) by the ethylene ketal in **1g** ($\theta = 12.0°$).[23] Figure 4 also rationalizes the 1.0 kcal/mol increase in the uncorrected magnitudes ΔE_{ST} between the optimized C_2 ($\theta = 12.0°$) and C_{2v} ($\theta = 0.0°$) geometries of **1g**.

The actual changes in the HOMO and LUMO energies of **1g** between $\theta = 12.0°$ and $\theta = 0.0°$, calculated at the RB3LYP/6-31G* level, are close to those expected from Figure 4. The energy difference between the HOMO energies at the optimized C_2 and C_{2v} geometries of **1g** was computed to be small, amounting to only 0.2 kcal/mol. In contrast, a significant difference of 1.6 kcal/mol was calculated between the LUMO energies at these two geometries. The sizable destabilization of the LUMO on decreasing θ by just 12.0° is consistent with the expected effect of increasing SC between n_O and ψ_A by increasing the overlap between these two orbitals.

The O−C2−O bond angle (ϕ) might also affect the size of ΔE_{ST} in 2,2-dialkoxycyclopentane-1,3-diyls, since this bond angle is calculated to be slightly smaller at the optimized geometry of singlet **1g** ($\phi = 104.4°$) than at those of **1d** ($\phi = 108.1°$) or **1e** ($\phi = 108.7°$). However, the effect of ϕ on ΔE_{ST} appears to be minimal. For example, the conformers of **1d** and **1e** with $\theta = 0°$ have optimized O−C−O bond angles of $\phi = 110.1°$ and $\phi = 119.1°$, both of which are considerably larger than the value of $\phi = 105.1°$ at the optimized C_{2v} geometry of **1g**. The values of $\Delta E_{ST} = -7.4$ and -7.2 kcal/mol calculated for **1d** and **1e**, respectively, at these geometries are quite close to the value of $\Delta E_{ST} = -7.6$ kcal/mol for **1g** at its optimized C_{2v} geometry.

Predicted Effect of the Ethylene-Ketal Functionality at C2 on the Electronic Spectra of Singlet Cyclopentane-1,3-diyls. Since singlet diradicals **2c**, **2d**, and **2f** are EPR-silent species at 77 K, an experimental test of the predicted effect of the ethylene ketal in **2g** on the size of the singlet−triplet energy gap is difficult. However, an experimentally accessible expression of the predicted effect of the ethylene ketal in **2g** on increasing the difference between the HOMO and LUMO energies should be found in the electronic absorption spectrum of **2g** when compared to the spectra of **2c**, **2e**, and **2f**.

As expected, when the electronic excitation energies were computed for the singlet diradicals **1**, we found a strong correlation between the calculated excitation energies and the calculated magnitudes of ΔE_{ST}. As shown in Table 1 and Figure 2, the computed excitation energies increase with decreasing O−C2−O−R dihedral angle (θ) in the same fashion as $|\Delta E_{ST}|$. The first strong absorption bands in the spectra ($f > 0.3$) are predicted to correspond to electronic excitation from the HOMO to the LUMO, and the absorption wavelengths (λ_{calcd}), calculated at the RCIS/6-31+G*//UB3LYP/6-31G* level of theory, decrease in the order **1e** (X = OCH_3) > **1g** (X,X = $-O(CH_2)_2O-$, C_2) > **1g** (C_{2v}) > **1c** (X = F).

Similar substituent effects on ΔE_{ST} and on the absorption bands are also predicted for the 1,3-diphenylcyclopentane-1,3-diyls **3** (Table 2). Both the RCIS and TD-RB3LYP/6-31G* methods predict that the λ_{calcd} decrease in the order of **3e** (X = OCH_3) > **3g** (X,X = $-O(CH_2)_2O-$) > **3c** (X = F).[24] This corresponds to the same type of blue shift that is predicted for the diradicals without phenyl substituents at C1 and C3.

We have already measured and reported the absorption spectra of **2c** and **2e**.[6b,c] Therefore, to test the prediction that the singlet diradical **2g** would absorb at longer wavelengths than **2c** but at

(24) For more accurate predictions of the UV−vis spectra of **3c**, **3e**, and **3g**, we would have liked to have performed calculations based on multireference CI or multireference perturbation theory. Unfortunately, such calculations, with appropriately large active spaces in the reference wave functions, were beyond the computational resources available to us.

Table 2. Calculated Substituent Effects on the Singlet−Triplet Energy Gaps (ΔE_{ST}) and on the Absorption Spectra of Singlet 1,3-Diphenylcyclopentane-1,3-diyls **3** and Absorption Wavelengths λ_{calcd} and Oscillator Strengths (f) Computed for the HOMO → LUMO Transition by the RCIS and TD-RB3LYP Methods. Absorption Wavelengths Calculated Are Compared to Those Observed (λ_{onset} and λ_{max}) for Singlet Diradicals **2**, Which Have a C4−C5 Propano Bridge That Is Absent in **3**

	diradical **3**						diradical **2**
			λ_{calcd}/nm				
			RCIS (f)[b]		TD-RB3LYP (f)[b]		
X		ΔE_{ST} in kcal/mol[a] ($\langle S^2_S\rangle$, ΔE_{ST}^{corr})	C_2	C_{2v}	C_2	C_{2v}	λ_{onset} (λ_{max}) in nm
F	**3c**	−4.7 (0.79, −7.7)		563 (1.27)		636 (0.55)	**2c** 580 (525)
OMe[c]	**3e**	−2.9 (0.90, −5.1)	720 (0.93)	657 (1.02)	859 (0.29)	754 (0.38)	**2e** 650 (571)
$-O(CH_2)_2O-$	**3g**	−4.6 (0.81, −7.6)	612 (1.03)	596 (1.16)	672 (0.44)	638 (0.53)	**2g** 590 (514)

[a] Calculations were performed at the UB3LYP/6-31G* level of theory. The values in parentheses indicate the $\langle S^2_S\rangle$ values for the singlet state and the energy gaps computed after correction for spin contamination in the singlet (ΔE_{ST}^{corr}) by using Yamaguchi's formula (ref 19); $\Delta E_{ST}^{corr} = \langle S^2_T\rangle/(\langle S^2_T\rangle - \langle S^2_S\rangle) \times \Delta E_{ST}$. The $\langle S^2_T\rangle$ values for the triplet state were calculated to be ca. 2.0 (see Supporting Information). [b] Calculated oscillator strengths. [c] At the C_2 minimum for singlet **3e**, the methyl groups are exo to the cyclopentane ring. However, at the C_{2v} global minimum, the methyl groups are endo to the cyclopentane ring, and this conformer was calculated to be 6.2 kcal/mol lower in energy than the C_2 geometry (see Supporting Information).

Scheme 1. Synthesis of Azoalkane **AZ**

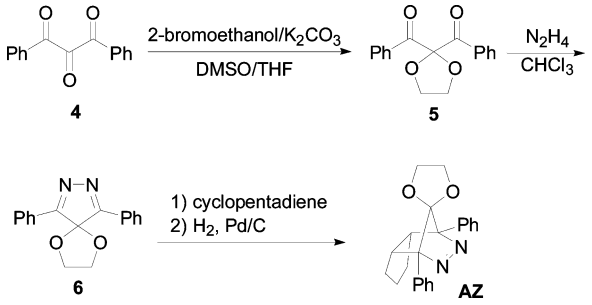

Scheme 2. Generation and Reaction of Singlet Diradical **2g**.

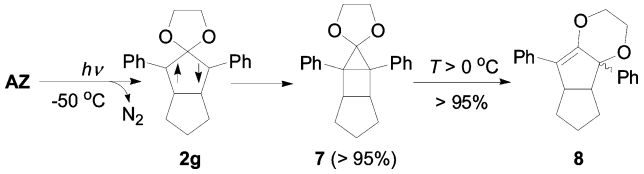

a significantly shorter wavelength than **2e**, we sought to generate **2g** and to obtain the electronic spectrum of this singlet diradical.

Generation of Singlet Diradical 2g. The precursor azoalkane **AZ** ($\lambda_{max} = 370$ nm, $\epsilon = 90$ M^{-1} cm^{-1} in benzene) was prepared by the method shown in Scheme 1. The photodenitrogenation of **AZ** was performed by irradiation with a 500W Xenon lamp ($\lambda_{irr} = 370 \pm 10$ nm), using a monochromator for wavelength selection. Photolysis of **AZ** in a degassed benzene solution at ca. 20 °C for 1 h, afforded a mixture of housane **7** and the two stereoisomers of the oxygen migration product **8** (Scheme 2). After allowing the photolysate to stand for 1 h at ca. 20 °C, the housane **7** was completely converted to **8**.

The photodenitrogenation was also performed at −50 °C in toluene-d_8, and direct analysis of the photolysate at −50 °C by ^{1}H and ^{13}C NMR spectroscopy revealed quantitative formation of the housane **7** (>95%). The housane **7** persisted below 0 °C, but at higher temperatures it was cleanly converted to rearrangement product **8**. For example, at 30 °C, the housane **7** completely disappeared within 45 min, with concomitant formation of **8** (Supporting Information, Figure S1). A similar rearrangement was observed in the experimental study of the singlet diradical **2c**.[6a]

Formation of housane **7** strongly suggests the intervention of diradical **2g** in the photodenitrogenation of **AZ**. To measure the electronic absorption spectrum of this putative singlet diradical intermediate, the photolysis of **AZ** was conducted in

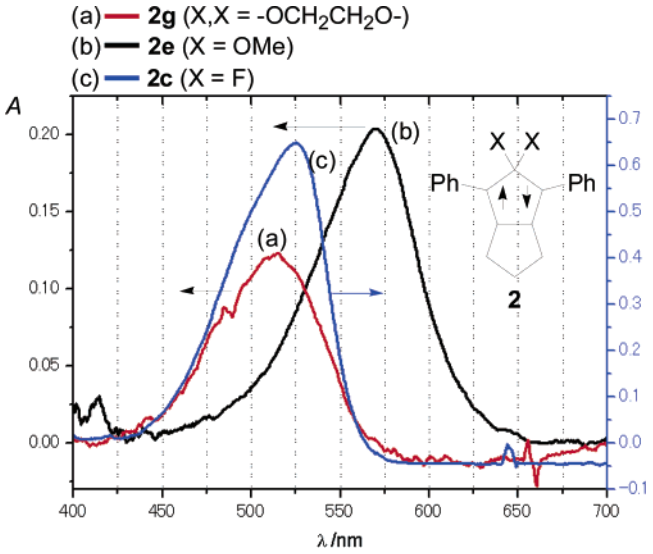

Figure 6. Experimental electronic absorption spectra of the singlet diradicals **2**, generated in the photodenitrogenation of the corresponding azoalkanes in MCH/MTHF glass at 77 K: (a) **2g** (X,X = $-O(CH_2)_2O-$), (b) **2e** (X = OMe), and (c) **2c** (X = F). The absorbance scale for spectra a and b is on the left side of the figure; that for spectrum c is on the right.

a methylcyclohexane (MCH)/2-methyltetrahydrofuran (MTHF) glass at 77 K ($\lambda_{irr} = 370 \pm 10$ nm). The resulting electronic absorption spectrum is shown in Figure 6a.

As predicted, the first band in the absorption spectrum of singlet **2g** ($\lambda_{max} = 514$ nm, $\lambda_{onset} = 590$ nm) exhibits a sizable blue shift when compared to that in the spectrum of singlet **2e** ($\lambda_{max} = 571$ nm, $\lambda_{onset} = 650$ nm, Figure 6b). The species that absorbs at $\lambda_{max} = 514$ nm was EPR-silent, as is the case for the singlet diradicals **2c** and **e**. This finding is consistent with the prediction that **2g**, like **2c** and **2e**, should have a singlet ground state.

The difluoro-substituted singlet diradical **2c** (X = F) was also generated. Its electronic absorption spectrum, obtained under conditions similar to those used to measure the spectrum of **2g**, showed $\lambda_{max} = 525$ nm and $\lambda_{onset} = 580$ nm (Figure 6c). We have previously reported the spectrum of **2c** in an EPA glass to have $\lambda_{max} = 530$ nm at 77 K.[6a]

The observed substituent effect on the band onsets ($\lambda_{onset} \approx \lambda_{0-0}$) for the diradicals **2** agrees well with the λ_{calcd} of the model diradicals **3** (Table 2). The RCIS computational method reproduces the experimental data especially well. The RCIS value of $\lambda_{calcd} = 657$ nm at the global energy minimum for **3e**

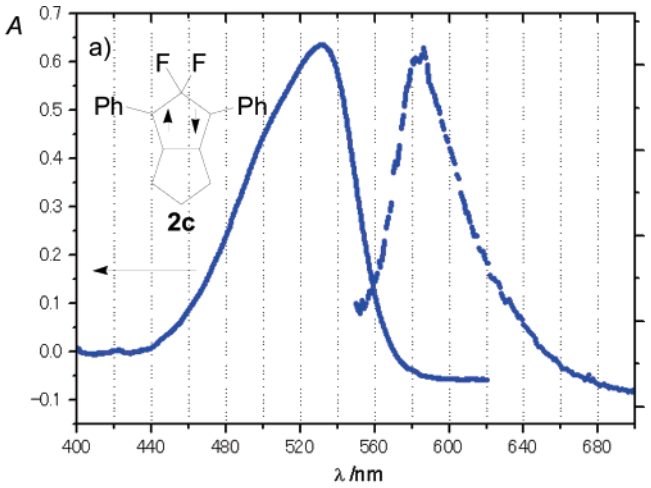

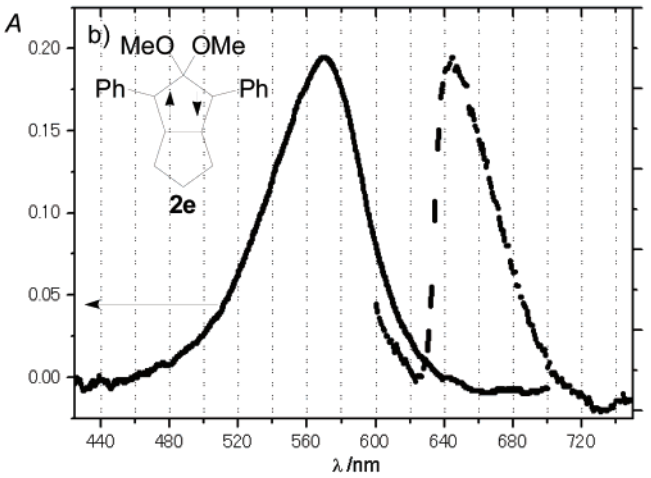

Figure 7. Electronic absorption spectra (solid line) and emission spectra (dashed line) of (a) the singlet diradical **2c** and (b) the singlet diradical **2e** in MCH/MTHF glass at 77 K.

(a C_{2v} geometry, in which both the methyl groups are endo to the cyclopentane ring) is quite close to the experimental value of λ_{onset} = 650 nm for **2e**.

Fluorescence emission, which mirrored the first electronic absorption band, was observed for **2c** (X = F, Figure 7a, λ_{exc} = 480 nm) and **2e** (X = OMe, Figure 7b, λ_{exc} = 540 nm) at 77 K. These emission bands clearly indicate that the observed absorption bands in the visible region are the lowest-energy electronic transitions of these two singlet diradicals. Fluorescence emission from **2g** (X,X = $-O(CH_2)_2O-$) was not detected under similar conditions, which suggests that the singlet diradical **2g** may be more photolabile than the singlet diradicals **2c** and **2e**.

The consistency between the theoretical predictions for the wavelengths of the HOMO → LUMO excitations in **1** (Table 1) and **3** (Table 2) and the experimental spectra of **2c**, **2e**, and **2g** (Figures 6 and 7 and Table 2) provides a sound basis for the reassignment of the visible absorption band of the singlet diradical **2c**. Although there were good arguments for assigning this strong, long-wavelength absorption to the excitation of an electron from the HOMO to the LUMO of the singlet diradical, the results of CASPT2 calculations of the excitation energy for this transition in 1,3-divinyl-2,2-difluorocyclopentane-1,3-diyl

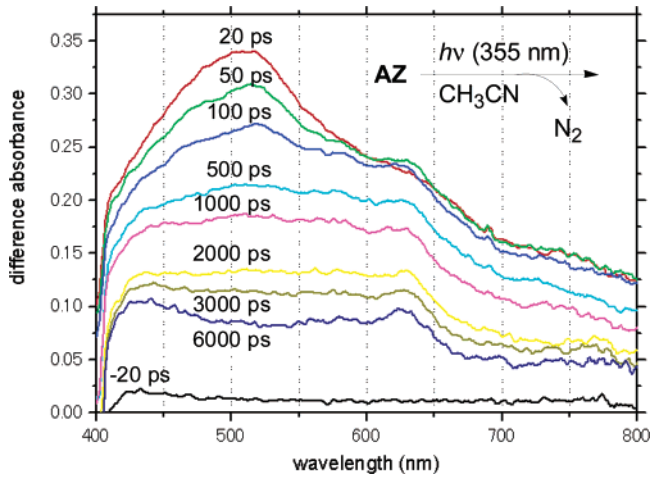

Figure 8. Transient electronic absorption spectra for the singlet diradical **2g** at the picosecond time scale (λ_{exc} = 355 nm, 20 ps pulse width).

(as a computationally tractable model for **2c**) argued against this assignment. The CASPT2 calculations predicted the HOMO → LUMO excitation in the divinyl model compound to occur at a significantly shorter wavelength than the absorption actually found in **2c**. These computational results, combined with the long-wavelength absorption that we found in the UV−vis spectrum of the ketyl radical, derived from 1,1,1-trifluoroacetophenone, led us tentatively to assign the strong absorption in **2c** to a parity-forbidden transition, largely localized in the benzyl chromophores.[6a]

To assess the effect of the ethylene-ketal unit on the lifetime of the singlet diradical, we also measured the lifetime of the transient absorption of **2g** at room temperature. No transient for **2g** was detected when a Q-switched Nd:YAG laser (λ_{exc} = 355 nm, 10 ns pulse width) was used for excitation of **AZ**. However, using a mode-locked laser (λ_{exc} = 355 nm, 20 ps pulse width) for excitation of **AZ** in acetonitrile led to the observation of a transient absorption. As shown in Figure 8, singlet diradical **2g** (λ_{max} = 510 nm) was formed within the duration of the laser pulse. The transient at 510 nm decayed with a lifetime of ca. 2 ns, leaving a broad absorption (415−650 nm), which decayed more slowly (6∼10 ns; see the 6000 ps spectrum in Figure 8). The latter species was not detected by nanosecond laser flash photolysis.

We cannot identify the second transient, but it might arise from a two-photon process, induced by the 20 ps laser pulse. As already noted, a high chemical yield (>95%) of the housane **7** was obtained upon preparative photolysis of **AZ** in acetonitrile at −20 °C (cf. Scheme 2). Therefore, it seems unlikely that the longer-lived transient is formed in significant yield by the same process that leads to the housane **7** in the preparative photolysis of **AZ**, unless, like diradical **2g**, the longer-lived transient also gives **7** in very high yield.

The lifetime of the singlet diradical **2g** (τ ca. 2 ns) is much shorter than those of **2e** (τ = 320 ns at 293 K in benzene) or **2f** (τ = 880 ns in benzene at 293 K and τ = 1.01 μs in acetonitrile at 293 K). The dramatic substituent effects on the lifetime of these singlet diradicals may be attributed to steric repulsion between the two phenyls and the alkoxy group that is cis to them in the transition state for cyclization. The effective size of the alkoxyl groups in **2f**, **2e**, and **2g** decreases in the order

EtO > MeO ≫ $-O(CH_2)_2O-$, and this is, in fact, the order in which the lifetimes of these three diradicals decrease.

Conclusion

Our calculations predict a strong correlation between the calculated singlet−triplet energy gaps in 2,2-disubstituted cyclopentane-1,3-diyls and the electronic excitation energies of these singlet diradicals. The combined theoretical and experimental data show that the ethylene-ketal functionality in **2g** (X,X = $-O(CH_2)_2O-$) exerts a powerful effect on both the ΔE_{ST} and the longest wavelength absorption in this singlet diradical. Our calculations indicate that spiroconjugation (SC) is responsible for the remarkable influence of the ketal group in **2g** on increasing $|\Delta E_{ST}|$ and on shifting the first absorption in the electronic absorption spectrum of this singlet diradical to shorter wavelengths. The present study provides a sound basis for reassignment of the strong absorption band of the singlet 2,2-disubstituted 1,3-diphenylcyclopentane-1,3-diyl derivatives **2** to excitation of an electron from the HOMO to the LUMO in each of these diradicals.

The HOMOs of these diradicals, which are formed from the symmetric combinations (ψ_S) of the π-NBMOs of the two benzylic moieties, are stabilized by hyperconjugation (HC) with the low-lying σ^* orbitals of the electronegative substituents, X, at C2. The LUMOs, which are formed from the antisymmetric combinations (ψ_A) of the benzylic NBMOs, are destabilized by spiroconjugation (SC) with the combination of lone pair orbitals on X that have the same symmetry as ψ_A. Both HC and SC contribute to making the singlet the theoretically predicted and experimentally found ground state of the diradicals **2c** and **2e**−**g**.

Experimental Section

Low-Temperature Spectroscopy. The electronic absorption spectra were measured at 77 K in a degassed MCH/MTHF glass by using a BAS USB2000 multichannel spectrophotometer. The fluorescence spectra were measured at 77 K on a HITACHI F2000 spectrophotometer.

Transient Absorption Spectroscopic Measurement. Nanosecond[25] and picosecond[26] time-resolved difference spectra were obtained by using the third harmonic of a Nd^{3+}:YAG laser (Continuum Surelite I-10, λ_{exc} = 355 nm) or of a mode-locked Nd^{3+}:YAG laser (Continuum PY61C-10, λ_{exc} = 355 nm) for excitation. White light from a Xe-arc lamp was used for acquisition of absorption spectra of species living longer than 10 ns. The transient absorption spectra in the time range from 20 ps to 6 ns were acquired by using continuum pulses with delays of 20−6000 ps. The latter were generated by focusing the fundamental laser pulse into a flowing H_2O/D_2O mixture (1:1 by volume).

Synthesis of Azoalkane AZ. 1,3-Diphenyl-2-ethlenedioxypropane-1,3-dione (5). A suspension of 1,3-diphenylpropanetrione **4** (9.00 g, 37.9 mmol) and 2-bromoethanol (2.7 mL, 37.9 mmol) in 18 mL of THF was mixed with K_2CO_3 (5.20 g, 37.9 mL) and 18 mL of DMSO. After stirring at 40 °C under an Ar atmosphere for 24 h, the yellow-brown solution was added to 100 mL of water. The organic layer was extracted with diethyl ether, dried over $MgSO_4$, and filtered. After the solvent was removed under reduced pressure (200 mmHg at 20 °C) on a rotary evaporator, the mixture was subjected to column chromatographic separation on silica gel (EtOAc/*n*-hexane = 10/90). The product **5** (7.00 g, 24.7 mmol, 65%) was obtained as a colorless powder after recrystallization from pentane−ether, mp 119−120 °C: IR (KBr) ν 1695 cm^{-1}; ^1H NMR (270 MHz, $CDCl_3$) δ 4.24 (s, 4 H), 7.36−8.09 (m, 10 H); ^{13}C NMR (67.8 MHz, $CDCl_3$) δ 66.5 (2 x t), 108.6 (s), 128.5 (4 x d), 130.2 (4 x d), 133.3 (2 x d), 133.9 (2 x d), 192.6 (2 x s). Anal. Calcd for $C_{17}H_{14}O_4$: C, 72.33; H, 5.00. Found: C, 72.10; H, 4.98.

4-Ethylenedioxy-3,5-diphenyl-4*H*-pyrazol (6). To a solution of **5** (6.6 g, 23.3 mmol) in $CHCl_3$ was added hydrazine monohydrate (1.13 mL, 23.3 mmol) under an Ar atmosphere. The mixture was refluxed for 24 h. After removal of the solvent (150 mmHg at 30 °C), the residue was subjected to silica gel chromatography (EtOAc/*n*-hexane = 20/80). Pyrazole **6** (1.50 g) was obtained together with some impurities: ^1H NMR (270 MHz, $CDCl_3$) δ 4.29 (s, 4 H), 7.44−7.88 (m, 10 H).

***endo*-10,10-Ethylenedioxy-1,7-diphenyl-8,9-diazatricyclo-[5.2.1.$0^{2,6}$]dec-8-ene (AZ).** The azo compound **AZ** was prepared from the pyrazole (1.50 g, 5.2 mmol) according to the Hünig route.[27] **AZ** (611 mg, 1.80 mmol, 35%) was obtained as colorless needles after recrystallization from methanol, mp 123−124 °C: IR (KBr) ν 2865−3090, 1498, 1473, 1445, 1120, 1035 cm^{-1}; ^1H NMR (270 MHz, $CDCl_3$) δ 1.35−1.74 (m, 6 H), 3.17 (t, J = 6.4 Hz, 2 H), 4.46 (t, J = 6.4 Hz, 2 H), 3.54−3.65 (m, 2 H), 7.35−7.83 (m, 10 H); ^{13}C NMR (67.8 MHz, $CDCl_3$) δ 25.7 (2 x t), 27.9 (t), 47.8 (2 x d), 65.1 (t), 65.7 (t), 93.7 (2 x s), 127.3 (s), 127.7 (4 x d), 128.0 (2 x d), 128.3 (4 x d), 134.8 (2 x s); UV (benzene) λ_{max} 370 nm (ϵ 90.2). Anal. Calcd for $C_{22}H_{22}N_2O_2$: C, 76.28; H, 6.40; N, 8.09. Found: C, 76.08; H, 6.31; N, 8.18.

Photodenitrogenation of Azoalkane AZ in Toluene-d_8. A solution of **AZ** (10.0 mg, 0.030 mmol) in toluene-d_8 (1 mL) was irradiated (λ_{exc} 370 ± 10 nm) for 3 h at −50 °C. The photolysate was directly analyzed by ^1H and ^{13}C NMR spectroscopy at −50 °C. Only housane **7** was detected under these conditions (>95%). After warming up to 30 °C, housane **7** was cleanly converted to the oxygen migration product **8**. **3,3-Ethylenedioxy-2,4-diphenyltricyclo[3.3.0.$0^{2,4}$]octane (7):** ^1H NMR (270 MHz, toluene-d_8) δ 1.42−1.52 (m, 3 H), 1.92−1.95 (m, 3 H), 3.15 (t, J = 6.5 Hz, 2 H), 3.20−3.22 (m, 2 H), 3.50 (t, J = 6.5 Hz, 2 H), 7.06−7.19 (m, 6 H), 7.30−7.33 (m, 4 H); ^{13}C NMR (67.8 MHz, toluene-d_8) δ 24.7 (t), 28.3 (2 x t), 41.1 (2 x d), 43.9 (2 x s), 64.3 (t), 64.4 (t), 103.1 (s), 125.2 (2 x d), 127.7 (4 x d), 129.6 (4 x d), 134.7 (2 x d).

Photolysis of the Azoalkane AZ on a Preparative Scale. A solution of **AZ** (180 mg, 0.52 mmol) in toluene (8 mL) was irradiated (λ_{exc} 370 ± 10 nm) for 15 h at 0 °C. After warming up to ca. 20 °C, the photolysate was stirred for 3 h in the dark. After removing the solvent (0.1 mmHg, 0 °C), the stereoisomeric rearrangement products, *endo*-**8** (46.0 mg, 32%) and *exo*-**8** (92.0 mg, 66%), were isolated as oils by using flash column chromatography on silica gel. The assignment of the configurations was performed by ^1H NMR NOE measurements.

(1*R,2*S**,6*R**)-1,7-Diphenyl-9,12-dioxatricyclo[6.4.0.$0^{2,6}$]dodec-7-ene (*endo*-8):** IR ν 3083, 3056, 2952, 2866, 1657, 1599 cm^{-1}; ^1H NMR (270 MHz, $CDCl_3$) δ 1.45−2.00 (m, 6 H), 2.43−2.51 (m, 1 H), 3.23−3.30 (m, 1 H), 3.68−4.03 (m, 4 H), 7.13−7.65 (m, 10 H); ^{13}C NMR (67.8 MHz, $CDCl_3$) δ 26.4 (t), 27.1 (t), 31.3 (t), 43.5 (d), 53.2 (d), 61.7 (t), 67.6 (t), 84.8 (s), 119.7 (s), 125.9 (2 x d), 126.4 (d), 127.0 (d), 127.8 (2 x d), 128.1 (2 x d), 128.6 (2 x d), 134.2 (d), 137.6 (s), 145.4 (s); Anal. Calcd for $C_{22}H_{22}O_2$: C, 82.99; H, 6.96. Found: C, 82.70; H, 7.04.

(1S*,2S*,6*R)-1,7-Diphenyl-9,12-dioxatricyclo[6.4.0.$0^{2,6}$]dodec-7-ene (*exo*-8):** IR ν 3088, 3056, 2954, 2866, 1658 cm^{-1}; ^1H NMR (270 MHz, $CDCl_3$) δ 0.78−1.82 (m, 6 H), 2.80−2.93 (m, 1 H), 3.55−3.94 (m, 5 H), 7.16−7.40 (m, 10 H); ^{13}C NMR (67.8 MHz, $CDCl_3$) δ 26.9 (t), 28.1 (t), 30.8 (t), 46.4 (d), 52.3 (d), 61.8 (t), 69.3 (t), 88.7 (s), 122.6 (s), 125.9 (d), 126.7 (d), 127.1 (2 x d), 127.8 (2 x d), 128.1 (2 x d), 128.2 (2 x d), 134.4 (s), 141.4 (s), 149.8 (s). Anal. Calcd for $C_{22}H_{22}O_2$: C, 82.99; H, 6.96. Found: C, 82.75; H, 7.01.

(25) Yoshimura, A.; Nozaki, K.; Ikeda, N.; Ohno, T. *J. Phys. Chem.* **1996**, *100*, 1630−1637.
(26) Ohno, T.; Nozaki, K.; Haga, M. *Inorg. Chem.* **1992**, *31*, 548−555.
(27) (a) Beck, K.; Hünig, S. *Chem. Ber.* **1987**, *120*, 477−485. (b) Nau, W. M.; Harrer, H. M.; Adam, W. *J. Am. Chem. Soc.* **1994**, *116*, 10972−10982.

Acknowledgment. The work in Osaka was supported by a grant-in-aid for Scientific Research from the Ministry of Education, Science, Sports, and Culture of Japan. We thank the Analytical Center of Faculty of Engineering, Osaka University. The work at the University of Würzburg was generously financed by the Deutsche Forschungsgemeinschaft, Volkswagen Foundation, Alexander-von-Humboldt Foundation, and the Fonds der Chemischen Industrie. The research at the University of Washington was funded by grants from the U.S. National Science Foundation. The work at Basel was supported by the Swiss National Science Foundation. Dr. Sheila Buxton is thanked for her help in the nomenclature for **AZ**, **7**, and **8**.

Supporting Information Available: Optimized geometries and energies for the diradicals **1** and **3** and low-temperature NMR spectra for product **7**. This material is available free of charge via the Internet at http://pubs.acs.org.

JA038305B